Phosphorylation Induces a Conformational Transition near the Lipid−Water Interface of Phospholamban Reconstituted with the Ca-ATPase[†]

Baowei Chen[‡] and Diana J. Bigelow*[,§]

School of Molecular Biosciences, Washington State University Tri-Cities, Richland, Washington 99352, and Pacific Northwest National Laboratory, P.O. Box 999, Richland, Washington 99352

Received August 9, 2002; Revised Manuscript Received September 19, 2002

ABSTRACT: We have measured conformational changes of phospholamban (PLB) induced both by its interaction with the SR Ca-ATPase and by phosphorylation of Ser-16 by cAMP-dependent protein kinase (PKA) using an engineered PLB having a single cysteine (Cys-24) derivatized with the fluorophore 2-(4′-maleimidylanilino)naphthalene-6-sulfonic acid (ANSmal). This modified mutant PLB is fully functional when co-reconstituted with the affinity-purified Ca-ATPase in liposomes. ANSmal emission properties and its solvent accessibility indicate that Cys-24 is in an aqueous environment outside the membrane. Fluorescence quenching and time-resolved anisotropy measurements of ANSmal-PLB demonstrate distinct structures for PLB in the free and Ca-ATPase-bound state. Both solvent exposure and probe motions of ANSmal are enhanced upon interaction of PLB with the Ca-ATPase. This conformational transition entails conversion of free PLB in a conformation which is insensitive to one which is sensitive to the phosphorylation state of PLB. Upon phosphorylation of Ca-ATPase-bound PLB, a decreased level of solvent exposure of ANSmal is observed, suggesting that the amino acid sequence of PLB near the lipid−water interface acts as a conformational switch in response to the phosphorylation of PLB. A longer correlation time, resolved by anisotropy measurements, corresponding to polypeptide chain fluctuations, is substantially restricted by interaction of PLB with the Ca-ATPase. This restriction is not reversed by phosphorylation of PLB, indicating that the region around Cys-24 near the lipid−water interface does not undergo dissociation from the Ca-ATPase. These results suggest that the phosphorylation by PKA induces a redistribution of PLB−Ca-ATPase protein contacts to relieve the inhibitory effect of PLB for the activation of calcium transport.

Phospholamban (PLB)[1] is a 52-residue integral membrane protein which is coexpressed with the cardiac/slow twitch isoform (SERCA2a) of the SR/ER Ca-ATPase. In the heart, this protein maintains the Ca-ATPase in an inhibited state at sub-micromolar calcium concentrations until it is phosphorylated at Ser-16 or Thr-17 by cAMP-dependent protein kinase or calmodulin-dependent protein kinase, respectively, in response to β-adrenergic stimulation (*1*−*6*). Phosphorylation of PLB results in activation of calcium transport across the SR and concomitant accelerated rates of muscle relaxation (*7*−*9*). This activation is manifested as a shift in the calcium concentration dependence of Ca-ATPase activity toward lower calcium concentrations (higher apparent affinity) relative to that of unphosphorylated PLB. The critical role of PLB in β-adrenergic responsiveness of both normal and diseased heart has stimulated considerable interest in elucidation of the physical mechanism by which PLB modulates Ca-ATPase activity.

Toward this goal, the availability of atomic resolution structures for both the Ca-ATPase and PLB has been a valuable tool for creating realistic models of PLB−Ca-ATPase interactions. For example, the determination of the crystal structure of the SERCA1 isoform of the Ca-ATPase has provided substantial insight into the three-dimensional structure of the cardiac isoform, SERCA2a (*10*). With its level of sequence identity to SERCA2a being 84%, SERCA1, in reconstituted liposomes, is identically regulated by the phosphorylation state of PLB; moreover, SERCA1 can functionally substitute for SERCA2a in the heart (*11*−*13*). In addition, the high-resolution structure of a monomeric mutant PLB (C41F) in its unphosphorylated form has been determined by NMR. While this structure was obtained in an organic solvent, it is in good agreement with secondary structural contents obtained by circular dichroism and Fourier transform infrared for native PLB in both reconstituted membranes and detergent micelles (*14*−*17*).

Along with the detailed structures of PLB and the Ca-ATPase, individually, structural information regarding their interactions with one another has come from mutagenesis experiments. These have identified specific amino acids

[†] This work was supported by grants from the National Institutes of Health (HL64031) and the American Heart Association.

* To whom correspondence should be addressed: Pacific Northwest National Laboratory, P.O. Box 999, Richland, WA 99352. Telephone: (509) 376-2378. Fax: (509) 376-1494. E-mail: diana.bigelow@pnl.gov.

[‡] Pacific Northwest National Laboratory.

[§] Washington State University Tri-Cities.

[1] Abbreviations: ATP, adenosine 5′-triphosphate; cAMP, adenosine 3′,5′-cyclic monophosphate; $C_{12}E_9$, polyoxyethylene 9-lauryl ether; EGTA, ethylene glycol bis(β-aminoethyl ether)-*N*,*N*,*N*′,*N*′-tetraacetic acid; OG, *n*-octyl β-D-glucopyranoside; ANSmal, 2-(4′-maleimidylanilino)naphthalene-6-sulfonic acid; MOPS, 3-(*N*-morpholino)propanesulfonic acid; PKA, cAMP-dependent protein kinase; PLB, phospholamban; POPOP, 1,4-bis(5-phenyl-2-oxazolyl)benzene; SDS−PAGE, sodium dodecyl sulfate−polyacrylamide gel electrophoresis; SERCA, sarco(endo)plasmic Ca-ATPase; SR, sarcoplasmic reticulum.

10.1021/bi0266030 CCC: $22.00
Published on Web 10/30/2002

within PLB and the Ca-ATPase that provide essential conformational features that are critical to their regulatory interaction based on the loss of the PLB-dependent shift in calcium activation of the Ca-ATPase when these residues are individually mutated (*18*−*22*). Interacting residues include the cytoplasmic sequence from Glu-2 to Ile-18 within PLB and DKKDPVK^{402} within SERCA2a. Of note, SERCA1 contains a nearly identical sequence, DKNDPIR^{402}, which may partially explain its ability to be regulated by PLB. Moreover, the wild-type amino acids Val-795, Leu-802, Thr-805, and Phe-809 which constitute one face of the transmembrane helix, M6, of the Ca-ATPase and those (Leu-31, Asn-34, Phe-35, Ile-38, Leu-42, Ile-48, Val-49, and Leu-52) within one face of the membrane-spanning helix of PLB are required for the inhibitory effect of PLB. The mechanism by which phosphorylation of Ser-16 or Thr-17 alters PLB structure within one or both of these interacting regions remains an area of active investigation. However, recent measurements have provided some insight via direct monitoring of binding interactions at the N-terminus of PLB and the Ca-ATPase with the use of spin-label EPR and fluorescence anisotropy (*11*). This study demonstrated that motional restriction, which is imposed within this region by interaction with the Ca-ATPase, is not reversed by phosphorylation at Ser-16, indicating that activation of the Ca-ATPase does not involve the disruption of binding interactions at the N-terminus of PLB. Similarly, a proton NMR study of the PLB peptide (residues 1−20) concluded that residues 1−8 of PLB remain associated with the Ca-ATPase following phosphorylation of Ser-16 (*23*).

Therefore, to investigate PLB−Ca-ATPase interactions further, we have probed a site on the C-terminal (membrane) side of the phosphorylation sites using an engineered PLB with a single cysteine at position 24, derivatized with the fluorophore 2-(4′-maleimidylanilino)naphthalene-6-sulfonic acid (ANSmal). On the basis of the high-resolution NMR structure of PLB, position 24 is located near the transition between the membrane-spanning helix and the connecting loop with the N-terminal cytosolic helix near a region of conformational disorder (Figure 1). The solvent accessibility and dynamics of a fluorophore at that position would be expected to be sensitive to structural transitions of PLB. From such measurements, we find evidence for distinct structures of PLB in association with the Ca-ATPase as compared with PLB alone. In addition, co-reconstitution of PLB with the Ca-ATPase induces restricted motional properties that reflect binding interactions with the Ca-ATPase; these interactions, while distinct from those at the N-terminus, also cannot be reversed by phosphorylation at Ser-16, indicating that transmembrane regions of Ca-ATPase and PLB do not dissociate with PLB phosphorylation. A preliminary presentation of this work was made at the 45th Annual Meeting of the Biophysical Society (*24*).

EXPERIMENTAL PROCEDURES

Materials. 2-(4′-Maleimidylanilino)naphthalene-6-sulfonic acid, sodium salt (ANS-mal), was purchased from Molecular Probes (Eugene, OR). Polyoxyethylene 9-lauryl ether ($C_{12}E_9$), cAMP-dependent protein kinase (PKA), cAMP, ATP, $MgCl_2$, the calcium ionophore A23187, EGTA, DEAE-cellulose, and *n*-octyl β-D-glucopyranoside (OG) were purchased from Sigma (St. Louis, MO). 3-(*N*-Morpholino)propanesulfonic acid (MOPS) was purchased from Fisher Biotech (Fair Lawn, NJ). Bio-Beads SM2 and acrylamide were purchased from Bio-Rad (Richmond, CA). DNA encoding the single-cysteine mutant phospholamban (PLB, Cys^{36,41,46}/Ala^{24}Cys) was cloned into a pGEX-2T plasmid expression vector, and expressed in JM 109 *Escherichia coli* cells. The expressed PLB protein was purified by preparative electrophoresis as previously described (*25*). Lipids were extracted from the SR vesicles isolated from rabbit skeletal fast-twitch muscle by standard methods (*26*, *27*). The Ca-ATPase was affinity purified from skeletal muscle SR using reactive red agarose (28).

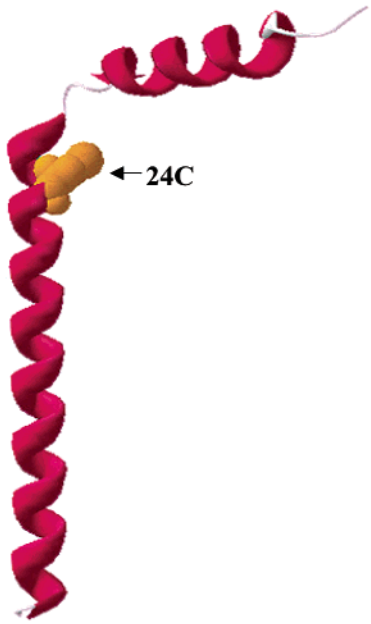

FIGURE 1: Position of ANSmal (represented as space-filling atoms) at Cys-24 within PLB based on the average NMR structure of C41F PLB in the nonphosphorylated form obtained in chloroform and methanol by Lamberth and co-workers (*14*).

Co-Reconstitution of the Ca-ATPase with PLB. Before reconstitution, the anionic detergent SDS in the purified PLB sample obtained from preparative SDS−PAGE was exchanged for the nonionic detergent $C_{12}E_9$ using DEAE-cellulose chromatography. This step involved application of approximately 2 mg of purified PLB in 10 mL of buffer containing 20 mM MOPS (pH 7.0) and 2.5% $C_{12}E_9$ onto a DEAE-cellulose column pre-equilibrated with the same buffer. PLB was eluted with 20 mM MOPS (pH 7.0), 2.5% $C_{12}E_9$, and 0.2 M NaCl. PLB was reconstituted in the absence or presence of purified Ca-ATPase at a final molar ratio of two PLBs per Ca-ATPase into liposomes of extracted SR lipids as previously described (*11*). The loss of fluorophores bound to the Ca-ATPase (FITC) or PLB (dansyl) following trypsin digestion of reconstituted vesicles indicated the asymmetry of these proteins in reconstituted membranes. The Ca-ATPase was found to be >95% asymmetrically (right-side out) reconstituted, while PLB was ~50% right-side out (essentially symmetrically reconstituted).

Enzymatic, Protein, and Free Calcium Assays. The ATP hydrolysis activity of the Ca-ATPase was determined by measuring the time course of the release of inorganic phosphate (29), using 100 μg of protein/mL in a solution at 25 °C containing 50 mM MOPS (pH 7.0), 0.1 M KCl, 5 mM $MgCl_2$, 1 mM EGTA, 2 μM A23187, and sufficient calcium to yield the desired concentration of free calcium.

ATP (5 mM) was added to start the reaction. To phosphorylate PLB for enzyme activity measurements, 10 μg of PKA/mL and 1 μM cAMP were also included in the assay buffer. All protein concentrations were determined by the amido black method (*30*). Free calcium concentrations were calculated from total ligand and EGTA concentrations, correcting for pH and ionic conditions (*31*).

Labeling with Spectroscopic Probes. Modification of the single-cysteine mutant PLB with ANSmal was carried out in a medium consisting of 20 mM MOPS (pH 7.0), 2.5% $C_{12}E_9$, and 0.2 M NaCl. Two milligrams of PLB was incubated with a 10-fold molar excess of ANSmal for 40 min in the dark at room temperature. Labeled PLB was separated from an unreacted probe using a Sephadex G-25 column. The level of incorporation of ANSmal was determined in a medium of 1% SDS and 0.1 M NaOH using a molar extinction coefficient ϵ_{330} of 2.0×10^4 M^{-1} cm^{-1} (*32*).

Steady-State Fluorescence Measurements. Fluorescence emission spectra of ANSmal were recorded with a FluoroMax-2 fluorometer (SPEX, Edison, NJ), using excitation and emission slits of 5 nm. Protein conformational changes were assessed by changes in the accessibility of ANSmal fluorescence to acrylamide. Quenching of probe bound to PLB for reconstituted samples was assessed by steady-state fluorescence intensities as a function of the acrylamide concentration at 25 °C in 50 mM MOPS (pH 7.0), 0.1 M KCl, 5 mM $MgCl_2$, 5 mM ATP, 1 mM EGTA, and 0.6 mM $CaCl_2$ (0.5 μM free calcium). To phosphorylate PLB, 40 μg/mL PKA and 1 μM cAMP were also included in the medium. These conditions ensure enzyme cycling during the course of the experiment, resulting in structural measurements of PLB in association with a time-averaged conformation of the Ca-ATPase rather than any single steady enzyme state. Data were analyzed as F_0/F as a function of the titrated acrylamide concentration and according to the Stern−Volmer equation:

$$F_0/F = 1.0 + K_{SV}[Q] \tag{1}$$

where F_0 and F are the fluorescence intensity in the absence and presence of added acrylamide, respectively. [Q] indicates the concentration of the quencher, acrylamide. K_{SV} values are products of both the fluorescence lifetimes in the absence of quencher (τ) and the bimolecular quenching constant (k_q), which is a true measure of solvent accessibility (*33*).

Frequency Domain Fluorescence. Frequency domain data (lifetime and anisotropy) were recorded using an ISS K2 frequency domain fluorometer described previously (*34*). Excitation utilized the 351 nm output from a Coherent (Santa Clara, CA) Innova 400 argon ion laser; emitted light was collected after it had passed through a GG420 long-pass filter, using 1,4-bis(5-phenyl-2-oxazolyl)benzene (POPOP) in methanol (lifetime of 1.35 ns) as a lifetime reference. Measurements were taken at 25 °C.

Analysis of Fluorescence Intensity and Anisotropy Decay. The frequency domain data were analyzed by a nonlinear least-squares method (*34*, *35*). The time-dependent decay $I(t)$ of fluorescence is generally fit to a sum of exponentials:

$$I(t) = \sum_{i=1}^{n} \alpha_i e^{-t/\tau_i} \tag{2}$$

where α_i values represent the pre-exponential factors, τ_i values represent the decay times, and n is the number of exponential components required to describe the decay. The intensity decay law is obtained from the frequency response of amplitude-modulated light and is characterized by the frequency-dependent values of the phase and the extent of demodulation. The values are compared with the calculated values from an assumed decay law until a minimum of the squared deviation (χ_R^2) is obtained. After the measurement of the intensity decay, the average lifetime was calculated:

$$\langle\tau\rangle = \frac{\sum_{i=1}^{n} \alpha_i \tau_i^2}{\sum_{i=1}^{n} \alpha_i \tau_i} = \sum_{i=1}^{n} f_i \tau_i \tag{3}$$

where f_i values represent the fractional intensities associated with each of the pre-exponential terms and $\langle\tau\rangle$ is directly related to the average time during which the fluorophore is in the excited state.

The frequency domain anisotropy decays [i.e., $r(t)$] were fit to a multiexponential model:

$$r(t) = r_0 \sum_{i=1}^{n} g_i e^{-t/\varphi_i} \tag{4}$$

where r_0 is the limiting anisotropy in the absence of rotational diffusion, φ_i is the rotational correlation time, $r_0 g_i$ represents the amplitude of the total anisotropy loss associated with each rotational correlation time, and n is the total number of components associated with the exponential decay (*36*). In all cases, parameter values are determined by minimizing the χ_R^2 which serves as a goodness-of-fit parameter that provides a quantitative comparison of the deviations between the measured and calculated values. Errors in the differential phase and modulated anisotropy were assumed to be 0.2 and 0.005, respectively.

Calculated Rotational Correlation Time for PLB in the Membrane. The overall dimensions of the membrane-spanning portion of PLB and the viscosity of the membrane (η) can be used to calculate the theoretical correlation time (ϕ_{calc}) for the overall rotational motion of PLB relative to the membrane normal according to the following equation (*37*, *38*):

$$\phi_{calc} = 2\pi\eta h a^2/kT \tag{5}$$

where h is the height and a the radius of the membrane-spanning portion of the protein, k is Boltzmann's constant, and T is the absolute temperature. SR membrane viscosity was previously determined to be 3.7 P at 25 °C (*39*). A value of 40 Å, the distance across a typical lipid bilayer, was used for h and 5 Å for a, the radius of the α-helix. These assumptions result in values of ϕ_{calc} of 1.1 μs for a PLB monomer and 10.2 μs for a PLB pentamer.

RESULTS

Native Functional Properties of ANSmal-Derivatized Single-Cysteine Mutant PLB Are Retained. A single-cysteine PLB mutant, designated (A24C)PLB, was constructed in

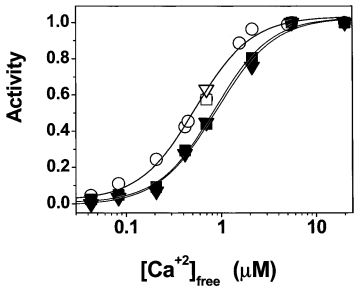

FIGURE 2: Calcium dependence of ATPase activity in reconstituted proteoliposomes. Proteoliposomes were composed of extracted SR lipids with affinity-purified rabbit skeletal Ca-ATPase without (○) or with (A24C)PLB (□ and ■) or ANSmal-PLB (△ and ▲). The symbols △ and □ designate the presence of 10 μg/mL PKA and 1 μM cAMP in the assay medium. ATPase activity was assayed at 25 °C, in a medium of 5 mM ATP, 80 mM KCl, 5 mM $MgCl_2$, 4 μM A23187, 1 mM EGTA, and 100 mM MOPS (pH 7.0). Activities are normalized relative to the maximal velocities [$V_{max} = 2.71 \pm 0.07$, 2.48 ± 0.06, and 1.75 ± 0.01 μmol of P_i min^{-1} (mg of protein)$^{-1}$ for the Ca-ATPase, Ca-ATPase with (A24C)PLB, and Ca-ATPase with ANSmal-(A24C)PLB, respectively]. All data were fit using the Hill equation. Values for the calcium concentration representing half-maximal activity (K_{Ca}) for the Ca-ATPase in the presence of (A24C)PLB and ANSmal-PLB are significantly higher ($K_{Ca} = 0.83 \pm 0.5$ and 0.87 ± 0.07 μM, respectively) than that of Ca-ATPase alone ($K_{Ca} = 0.50 \pm 0.06$ μM). Phosphorylation of PLB with PKA results in a shift in the calcium dependence of Ca-ATPase activity to a lower free calcium concentration.

which the three transmembrane cysteines (Cys-36, Cys-41, and Cys-46) of wild-type PLB were substituted with alanines, and a further substitution was introduced (a cysteine for Ala-24). Expression and purification of this PLB mutant from *E. coli* were followed by its covalent modification with the thiol-reactive fluorophore ANSmal (designated ANSmal-PLB), and reconstitution into liposomes in the absence or presence of affinity-purified Ca-ATPase. The fast-twitch skeletal muscle sarcoplasmic/endoplasmic reticulum Ca-ATPase isoform (SERCA1) was used in these experiments on the basis of its stability in the detergents required for its purification and reconstitution (*28*). Reconstitution results in tightly sealed liposomes that are fully capable of ATP hydrolysis coupled to calcium transport (Figure 2). The Ca-ATPase exhibits cooperative calcium activation curves fitting to the Hill equation in the absence or presence of co-reconstituted (A24C)PLB or ANSmal-PLB. Values for the calcium concentrations required for half-maximal activation of the Ca-ATPase (K_{Ca}) in the absence and presence of PLB and the extent of the PLB-induced shift (ΔK_{Ca}) in these values toward higher calcium concentrations (0.33 μM) are in good agreement with those derived for wild-type PLB in both reconstituted and native cardiac SR membranes (*25*, *40*). Moreover, phosphorylation of either mutant or fluorophore-modified PLB by PKA completely reverses this functional inhibition at sub-micromolar calcium concentrations. Thus, the inhibitory interaction between ANSmal-PLB and the SERCA1 isoform of the Ca-ATPase in these reconstituted preparations provides a reliable in vitro model, both qualitatively and quantitatively, for SERCA2a regulation by PLB in native cardiac SR.

ANSmal-Derivatized Cys-24 Is Not Incorporated into the Bilayer. In all current structural models of PLB, the 24 position is located at or near the membrane surface, where residues 27−52 provide a helix of sufficient length to span the 40 Å membrane bilayer (*15*, *41*). The sensitivity of ANS

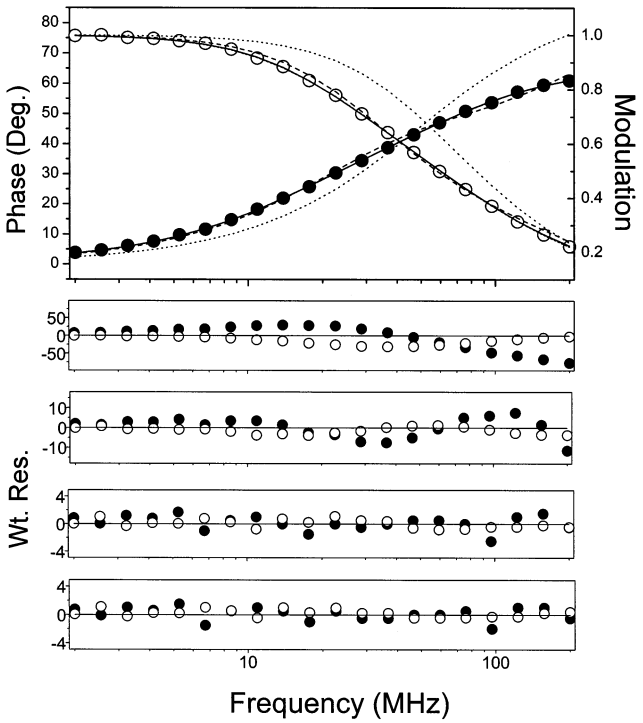

FIGURE 3: Frequency response of the phase shift and modulation of the emission of ANSmal after excitation with intensity-modulated light at different frequencies between 2 and 200 MHz. Emission was measured for ANSmal-PLB co-reconstituted with the Ca-ATPase in the SR lipids at 25 °C. Data are shown for ANSmal-PLB for the phase shift (●) and modulation (○). The fits correspond to one (···), two (- - -), and three (—) exponential components; a four-exponential fit can be superimposed on that for three exponentials. Weighted residuals (phase and modulation) are shown in the panels below the frequency domain data, and from top to bottom, corresponding to one-, two-, three-, and four-exponential fits to the data. The weighted residuals correspond to the difference between the experimental data and the calculated fit divided by the standard error of the individual measurement, assumed to be 0.20 and 0.005 for phase and modulation data, respectively. The reduced χ^2 (χ_R^2) values for the fits are 726, 15.1, 0.8, and 0.6 for one-, two-, three-, and four-exponential models, respectively. Lifetime measurements were taken in a medium containing 50 mM MOPS (pH 7.0), 0.1 M KCl, 5 mM $MgCl_2$, 5 mM ATP, 1 mM EGTA, and 0.6 mM $CaCl_2$ ($[Ca^{2+}]_{free} = 0.6$ μM).

emission to solvent effects provides a means of directly probing the environment around this bound fluorophore. The maximal emission wavelength of bound ANSmal ($\lambda_{max} =$ 420 nm) is characteristic of ANS bound to protein and distinctly blue-shifted relative to that for ANSmal ($\lambda_{max} =$ 442 nm) in water or at the polar membrane surface (*42*, *43*). No spectral shifts are detected under any of the experimental conditions used in this study, suggesting that neither Ca-ATPase interaction nor phosphorylation of PLB alters the environment around Cys-24 in such a way that would involve its partitioning into lipid or aqueous phases.

Fluorescence Lifetime Measurements. Time-resolved emission decays are particularly sensitive to the environment around the probe, often exhibiting changes when spectral shifts are not evident. Therefore, fluorescence lifetimes of ANSmal-PLB were obtained from the frequency modulation method (Figure 3). The intensity decays for all samples are adequately described as the sum of three exponentials, as shown by the random distribution of the weighted residuals and relative reduction in χ^2 values relative to those for simpler models. As illustrated in Figure 3 for ANSmal-PLB

Table 1: Lifetime Data for ANSmal-PLB Reconstituted in the Presence and Absence of the Ca-ATPase[a]

sample	condition	α_1	τ_1 (ns)	α_2	τ_2 (ns)	α_3	τ_3 (ns)	$\langle\tau\rangle$ (ns)
PLB	without PKA	0.53 (0.03)	0.69 (0.03)	0.33 (0.04)	2.7 (0.3)	0.15 (0.01)	8.3 (0.7)	5.2 (0.3)
	with PKA	0.41 (0.10)	0.99 (0.50)	0.44 (0.15)	2.0 (0.9)	0.16 (0.01)	7.9 (0.2)	4.9 (0.4)
PLB with Ca-ATPase	without PKA	0.47 (0.08)	0.65 (0.06)	0.34 (0.04)	2.7 (0.7)	0.20 (0.04)	8.0 (0.7)	5.5 (0.3)
	with PKA	0.54 (0.04)	0.69 (0.07)	0.32 (0.01)	3.3 (0.4)	0.15 (0.01)	8.7 (0.1)	5.6 (0.2)

[a] Lifetime measurements were taken in medium containing 50 mM MOPS (pH 7.0), 0.1 M KCl, 5 mM $MgCl_2$, 5 mM ATP, 1 mM EGTA, and 0.6 mM $CaCl_2$ in the presence and absence of 40 μg/mL PKA and 1 μM cAMP with excitation at 351 nm using a GG 420 filter. Average amplitudes (α_i) and lifetimes (τ_i) were obtained from three-exponential fits to the frequency domain. $\langle\tau\rangle$ is the average lifetime. Errors are standard deviations of two independent measurements.

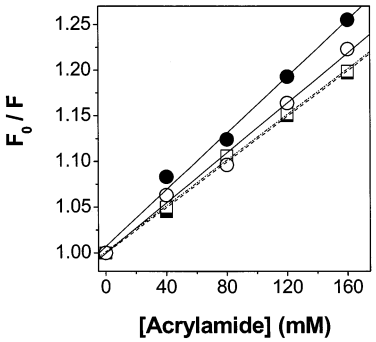

FIGURE 4: Acrylamide quenching of ANSmal-PLB reconstituted in SR lipids in the absence (□ and ■) and presence of the Ca-ATPase (○ and ●) either before (● and ■) or following phosphorylation by PKA (○ and □). Quenching was measured as fluorescence intensities (F) relative to that of the unquenched sample (F_0) at various acrylamide concentrations. Samples consisted of 50 or 15 μg/mL reconstituted membrane protein in the absence or presence of 40 μg/mL PKA and 1 μM cAMP in 50 mM MOPS (pH 7.0), 0.1 M KCl, 5 mM $MgCl_2$, 5 mM ATP, 1 mM EGTA, and 0.6 mM $CaCl_2$ ($[Ca^{2+}]_{free}$ = 0.6 μM). Fluorescence was measured at 420 nm with excitation at 320 nm using a GG 400 filter. Data points represent the means of three measurements of one reconstituted sample under the indicated conditions.

co-reconstituted with the Ca-ATPase, a 20-fold improvement in the goodness of fit (i.e., χ_R^2) is observed for a model involving three exponentials relative to that for two exponentials, whereas a four-exponential model does not significantly improve the fit. Thus, the three-exponential model is statistically justified. Best fit values for amplitudes and lifetime components are shown in Table 1 for ANSmal-PLB reconstituted in the absence and presence of the Ca-ATPase as well as before and following PKA-induced phosphorylation of PLB. Neither the average lifetimes ($\langle\tau\rangle$) nor the contributing amplitudes (α_i) and lifetime components (τ_i) of ANSmal-PLB are significantly altered by interaction with the Ca-ATPase or by phosphorylation at Ser-16. Thus, the more sensitive lifetime data are consistent with the spectral data in indicating no large changes in the polarity around ANSmal.

Changes in the Solvent Accessibility of ANSmal-Modified PLB. We find evidence for conformational changes around Cys-24 induced by both interaction of PLB with the Ca-ATPase and PLB phosphorylation that can be detected by changes in the accessibility of bound ANSmal to acrylamide, a water-soluble quencher of fluorescence (Figure 4 and Table 2). As is characteristic of protein-bound fluorophores, substantial protection of PLB-bound ANSmal from quenching by acrylamide as is observed compared with that of ANSmal free in solution, as evidenced by the K_{SV} values obtained from slopes of Stern−Volmer plots (Table 2). On the other hand, co-reconstitution of PLB with the Ca-ATPase

Table 2: Solvent Accessibilities of ANSmal-PLB Reconstituted in the Presence and Absence of Ca-ATPase[a]

sample	condition	K_{SV} (M^{-1})[b]
PLB	control	1.25 ± 0.04
	with PKA	1.25 ± 0.05
PLB with Ca-ATPase	without PKA	1.40 ± 0.09
	with PKA	1.24 ± 0.06
ANSmal		3.27 ± 0.12

[a] Measurements were taken for reconstituted samples in the absence or presence of 40 μg/mL PKA and 1 μM cAMP in 50 mM MOPS (pH 7.0), 0.1 M KCl, 5 mM $MgCl_2$, 5 mM ATP, 1 mM EGTA, and 0.6 mM $CaCl_2$. The fluorescence was measured at 420 nm with excitation at 320 nm with a GG 400 filter. K_{SV} values represent averages and propagated errors of three independent measurements each for four separately reconstituted samples. [b] K_{SV}, the slope of the Stern−Volmer plot, was obtained from the relationship $F_0/F = 1.0 + K_{SV}[Q]$, where F_0 and F are the fluorescence intensities in the absence and presence of added quencher, respectively, and [Q] is the concentration of quencher added.

results in increased accessibility of ANSmal to quenching when PLB is unphosphorylated; PKA-mediated phosphorylation of PLB results in the reversal of this effect. Thus, interaction of PLB with the Ca-ATPase has two effects: (1) rendering the solvent accessibility of Cys-24 sensitive to the phosphorylation state of PLB and (2) increasing the solvent accessibility of bound ANSmal in the unphosphorylated state. The latter observation suggests a more open structure around Cys-24 when PLB is bound to the Ca-ATPase relative to that of free PLB. K_{SV} values are a product of both solvent accessibility, i.e., the bimolecular quenching constant (k_q), and the fluorescence lifetime of the fluorophore; thus, the previous observation that the lifetime of bound ANSmal is unchanged under any of the experimental conditions that were used (Table 1) indicates that the observed changes in K_{SV} values are entirely a result of changes in solvent accessibility.

Fluorescence Anisotropy Measurements of PLB Rotational Dynamics. Anisotropy measurements of protein dynamics have been used to recover information regarding protein structure, conformational changes, and protein−protein interactions (*44*). Anisotropy decays of ANSmal-PLB were examined in the absence and presence of the Ca-ATPase using frequency domain fluorescence. Data were collected over 20 frequencies between 2 and 200 MHz (Figure 5), and the data were fit to a sum of exponentials using previously described algorithms (*41*, *46*). In all cases, the fluorescence anisotropy decays of ANSmal-PLB were adequately fit to a model consisting of two exponentials as judged by both the 50-fold reduction in χ_R^2 and the evenly distributed residuals. Additional fitting parameters result in no improvement in the calculated fit to the data. The initial anisotropy (r_0 = 0.36 ± 0.05) is close to the theoretical maximum of 0.4,

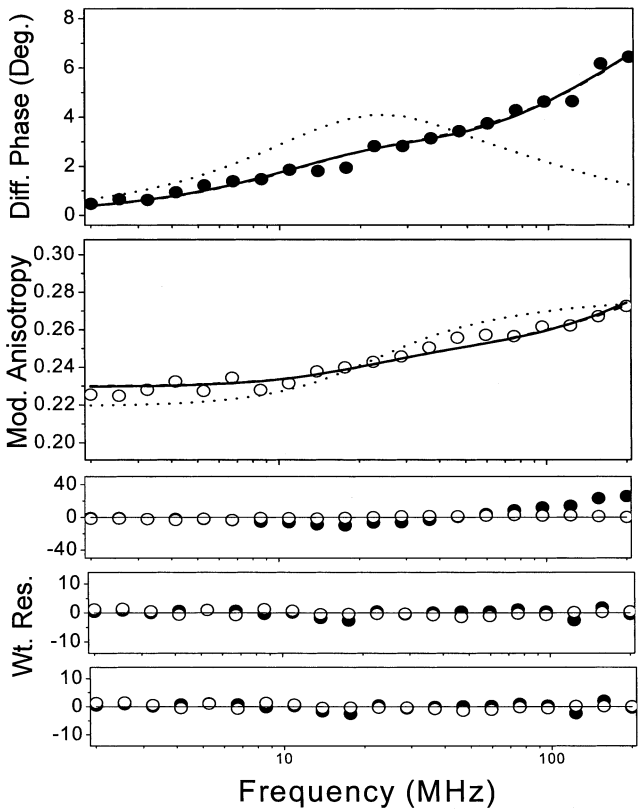

FIGURE 5: Frequency domain fluorescence anisotropy data for ANSmal-PLB co-reconstituted with the Ca-ATPase in the SR lipids at 25 °C. Data are shown for ANSmal-PLB for the differential phase angle (●) and modulated anisotropy (○). The fits correspond to one (···), two (—), and three (- - -) exponential components. Weighted residuals, from top to bottom, correspond to one-, two-, three-exponential fits to the data. The weighted residuals correspond to the experimental data minus the calculated value for the multiexponential fits normalized by the standard errors for the measurements, which were assumed to be 0.20 and 0.005 for the differential phase and modulated anisotropy, respectively. The reduced χ^2 (χ_R^2) values for the fit of ANSmal-PLB are 54.1, 1.1, and 1.0 for one-, two-, and three-exponential models, respectively. The measurements were taken in medium containing 50 mM MOPS (pH 7.0), 0.1 M KCl, 5 mM $MgCl_2$, 5 mM ATP, 1 mM EGTA, and 0.6 mM $CaCl_2$ ($[Ca^{2+}]_{free} = 0.6$ μM).

indicating that the majority of the fluorescence anisotropy decay has been resolved. With this nearly rigid binding of ANSmal to Cys-24 of PLB, it is to be expected that protein dynamics can be resolved from the anisotropy decay with little contribution from motions associated with probe flexibility (59−62). Data from rotational dynamic measurements of ANSmal-PLB are shown in Table 3 for either PLB alone or PLB after co-reconstitution with the Ca-ATPase. In both cases, two correlation times were resolved, the subnanosecond ϕ_1, corresponding to local (side chain and probe) dynamics, and the 100-fold longer ϕ_2, representing internal dynamics of the PLB polypeptide chain. The measured ϕ_2 is too short to represent the overall motion of PLB coupled with its transmembrane domain, which, calculated on the basis of the dimensions of PLB and the membrane viscosity, is 1.1 μs for a PLB monomer (see eq 5 in Experimental Procedures). Thus, ϕ_2 indicates that Cys-24 is in a conformationally disordered region of the protein.

The rate of the local motion ($1/\phi_1$) increases upon association of PLB with the Ca-ATPase, consistent with the more open structure around ANSmal indicated by its greater solvent accessibility (Figure 4 and Table 2). However, only small changes in the rate and amplitude of this motion are detected upon phosphorylation of PLB, indicating that phosphorylation does not reverse local motional changes, in contrast to the effect of phosphorylation on solvent accessibility. In the case of internal protein dynamics, Ca-ATPase interaction with PLB results in a decreased rate ($1/\phi_2$) without changes in the amplitude (g_2r_0) of this motion (Table 3). This substantial motional restriction of the PLB polypeptide resulting from Ca-ATPase interaction is not reversed by phosphorylation of PLB, indicating that regulation of the Ca-ATPase does not involve phosphorylation-induced disruption of protein−protein associations between the region around Cys-24 of PLB and the Ca-ATPase.

DISCUSSION

Most of the structural information available for PLB has been derived from studies of either PLB peptides or the entire PLB protein in isolation rather than in association with the Ca-ATPase (*14*−*16*, *41*, *45*−*50*). The requirement for a conformational signal unique to PLB in the presence of the substantially larger Ca-ATPase is satisfied, in our study, by the combined use of mutagenesis and fluorescence spectroscopy. The ANSmal-derivatized single-cysteine mutant PLB used for this study has provided a reliable probe of PLB structure from the perspective of a site near the region of conformational disorder and without perturbation of the normal function of PLB. The fluorophore-modified mutant PLB, after co-reconstitution, provides both inhibition of the Ca-ATPase, at sub-micromolar calcium concentrations, and its activation after PKA-induced phosphorylation of PLB, which is quantitatively identical to that of wild-type PLB in native cardiac SR membranes (Figure 2; *40*). It should be pointed out that while the Ca-ATPase reconstitutes asymmetrically with a right-side out orientation, PLB reconstitutes essentially symmetrically (see Experimental Procedures; *11*). Thus, the two PLBs per ATPase used in these reconstituted proteoliposomes ensure full regulation of all Ca-ATPase, as evidenced by the maximal shift in calcium activation (Figure 2). The presence of a population of ANSmal-PLB which is not accessible to quencher or to PKA-induced phosphorylation suggests that these fluorescence measurements underestimate the structural changes induced by phosphorylation of PLB or interaction with the Ca-ATPase.

Table 3: Rotational Dynamics of ANSmal-PLB Reconstituted in the Presence and Absence of the Ca-ATPase[a]

sample	condition	g_1r_0	ϕ_1 (ns)	g_2r_0	ϕ_2 (ns)
PLB	control	0.10 ± 0.03	0.55 ± 0.18	0.24 ± 0.03	32 ± 5
PLB with Ca-ATPase	without PKA	0.15 ± 0.01	0.14 ± 0.01	0.24 ± 0.01	76 ± 7
	with PKA	0.11 ± 0.02	0.21 ± 0.04	0.25 ± 0.02	77 ± 7

[a] Sample conditions are as described in the frequency domain fluorescence experiments. g_ir_0 values are the amplitudes of the total anisotropy associated with each rotational correlation time (ϕ_i). ϕ_1 and ϕ_2 are the rotational correlation times associated with segmental and overall protein rotational motion, respectively. Errors are standard deviations of measurements from two separate reconstituted samples.

Probing the Local Environment around Cys-24. The environmentally sensitive fluorescence properties of ANSmal indicate its solvation within the PLB protein structure rather than in lipids or water, consistent with a position of Cys-24 outside of the membrane. From characterization of the local environment around Cys-24 comes evidence for distinct structures for PLB alone as compared with PLB in association with the Ca-ATPase. Specifically, quenching studies demonstrate a substantial increase in the level of solvent exposure of bound ANSmal as a result of the interaction between PLB and the Ca-ATPase, suggesting that the Ca-ATPase induces PLB to adopt a conformation involving a more open structure around Cys-24 (Figure 2 and Table 2). Consistent with this, and as might be expected by a less constrained probe environment, we observe an increase in the rate ($1/\phi_1$) of local probe motion induced by interaction with the Ca-ATPase (Figure 5 and Table 3). Current knowledge of PLB structure suggests two conformational transitions that might explain these results. For example, the monomeric C41F PLB structure in an organic solvent, resolved by NMR, consists of two helices, between amino acids 4−16 and residues 21−49, connected by a β-turn ($TIEM_{20}$) which forms a flexible bend in the PLB structure (*14*). It is feasible that extension of this bent conformation is required for accommodation of the binding of N-terminal residues of PLB to the $DKNDPIR^{402}$ motif of the Ca-ATPase which is located relatively high (∼40 Å) above the bilayer surface (*10*, *14*, *22*). Such an extension of the PLB structure would result in a more open conformation around ANSmal (Figure 1). Alternatively, ANSmal may occupy an occluded location within an oligomeric form of free PLB; dissociation of PLB into monomers that interact with the Ca-ATPase would result in greater level of exposure of ANSmal to solvent. This explanation would seem to be the less likely one based on mutagenesis and modeling studies that predict the structure for the predominant oligomeric form of free PLB, the pentamer (*49*, *51*, *52*). From this model, in which the pentamer is formed by a series of leucine zippers between adjacent faces of the membrane-spanning helices of PLB monomers, Cys-24 is positioned on the outside surface of the pentamer, where it is exposed to solvent rather than buried within the pentameric structure. Distinct conformations for free and bound forms of PLB are also evidenced from the observation that the local environment of free PLB is insensitive to the phosphorylation state of PLB, while PLB bound to the Ca-ATPase shows a marked decrease in solvent accessibility of ANSmal upon phosphorylation of PLB (Figure 4 and Table 2). These results suggest that the structure of PLB in isolation may not be entirely relevant to the regulation of the Ca-ATPase and highlights the need for structural information regarding PLB complexed with the Ca-ATPase.

Polypeptide Chain Dynamics Are Sensitive to Protein−Protein Interactions. Additional structural information is available from the resolution of slower protein motions (ϕ_2) associated with polypeptide chain fluctuations (Figure 5 and Table 3). It is of interest to compare the motional properties of this probe at Cys-24 with those previously measured at the N-terminus of PLB (*11*). The anisotropy decay at the N-terminus, in both the free and Ca-ATPase-bound forms of PLB, is described well by two correlation times (of 1 and 9 ns each) with a large residual anisotropy that indicates a highly ordered structure at the N-terminus of PLB. On the other hand, explicit fitting of the anisotropy decay of ANSmal at Cys-24 of PLB to a similar model (having a residual anisotropy) results in a poor fit relative to that shown in Table 3. Thus, these results indicate that the protein structure at the C-terminal end of the cytoplasmic domain of PLB exhibits more motional freedom and is less ordered than that at the N-terminal end, as might be expected for the region around Cys-24 which borders the disordered loop region of the $TIEM_{20}$ motif. Despite these differences, protein motion in both regions of PLB is substantially restricted by interaction with the Ca-ATPase, indicating the presence of protein contacts in both regions. Significantly, this restriction is not reversed by phosphorylation of PLB, suggesting that the relief of Ca-ATPase inhibition results from neither complete dissociation of PLB from the Ca-ATPase nor disruption of PLB−Ca-ATPase contacts at the C- and N-terminal ends of the cytoplasmic domain of PLB. Rather, it is more likely that phosphorylation of PLB results in a redistribution of protein interactions involving only transient disruptions of protein contacts.

This latter result is in agreement with recent NMR and immunoprecipitation data demonstrating that phosphorylation of PLB does not disrupt association of a cytoplasmic PLB peptide (residues 1−25) from the ATPase in membranes or immunoprecipitation of PLB and the ATPase in detergent micelles. These recent results contradict commonly held models of association−dissociation mechanisms based on early cross-linking data (*3*, *22*, *23*, *53*−*56*). In view of these recent data, the previous observation of a phosphorylation-induced loss of cross-linking by a photoaffinity label on Lys-3 of PLB to the Ca-ATPase suggests structural changes of PLB that result in suboptimal reactivity of the already low-efficiency cross-linker. A more recent study demonstrates high-efficiency cross-linking with 1,6-bismaleimidohexane between the ATPase and position 30 of PLB, which is largely retained following phosphorylation of Ser-16 of PLB (*57*). Interestingly, this site is on the C-terminal side of Cys-24 and at the putative interface of the membrane-spanning domain (residues 31−52) of PLB, suggesting that this region, too, may remain associated with the ATPase during the regulatory cycle. A regulatory mechanism involving a phosphorylation-induced redistribution of protein−protein contacts is consistent with the reversal of the PLB-induced stabilization of helical elements of the Ca-ATPase observed by FTIR and the associated restriction in the amplitude of catalytically important motions within the nucleotide binding domain observed from anisotropy measurements (*12*, *58*). These restrictions in dynamics of structural elements within the Ca-ATPase, in turn, lead to a restriction in the entire array of protein motions involved in catalysis with the associated larger activation barrier for calcium activation and the associated nucleotide utilization (*59*).

Conclusions and Future Directions. We have identified a conformational transition involving position 24 in PLB associated with the phosphorylation of PLB and the release of the inhibitory interaction between PLB and the Ca-ATPase. This region is close to a disordered region previously identified by NMR spectroscopy, and probably part of a conformational switch that modulates the inhibition of the Ca-ATPase by PLB. Changes in this region may alter

the structural coupling between cytosolic and membrane-spanning regions of PLB that interact with the Ca-ATPase. Future studies should further explore the dynamic structure of this disordered region of PLB to identify how changes in protein structure affect the inhibition of the Ca-ATPase.

ACKNOWLEDGMENT

We thank Dr. Qing Yao for construction of the A24C-PLB mutant used in this study and Dr. Thomas C. Squier for helpful discussions.

REFERENCES

1. Tada, M., Kirchberger, M. A., and Katz, A. M. (1975) *J. Biol. Chem. 250*, 2640−2647.
2. Inui, M., Chamberlain, B. H., Saito, A., and Fleischer, S. (1986) *J. Biol. Chem. 261*, 1794−1800.
3. James, P., Inui, M., Tada, M., Chiesi, M., and Carafoli, E. (1989) *Nature 342*, 90−92.
4. Kranias, E. G. (1985) *J. Biol. Chem. 260*, 11006−11010.
5. Wegener, A. D., Simmerman, H. K. B., Lindemann, J. P., and Jones, L. R. (1989) *J. Biol. Chem. 264*, 11468−11474.
6. Simmerman, H. K. B., and Jones, L. R. (1998) *Physiol. Rev. 78*, 921−947.
7. Lindemann, J. P., Jones, L. R., Hathaway, D. R., Henry, B. G., and Watanabe, A. M. (1983) *J. Biol. Chem. 258*, 464−471.
8. Sasaki, T., Inui, M., Kimura, Y., Kuzuya, T., and Tada, M. (1992) *Biol. Chem. 267*, 1674−1679.
9. Stokes, D. L. (1997) *Curr. Opin. Struct. Biol. 8*, 550−556.
10. Toyoshima, C., Nakasako, M., Nomura, H., and Ogawa, H. (2000) *Nature 405*, 647−655.
11. Negash, S., Yao, Q., Sun, H., Li, J., Bigelow, D. J., and Squier, T. C. (2000) *Biochem. J. 351*, 195−205.
12. Tatulian, S. A., Chen, B., Li, J., Negash, S., Middaugh, C. R., Bigelow, D. J., and Squier, T. C. (2002) *Biochemistry 41*, 741−751.
13. Ji, Y., Loukianov, E., Loukianov, T., Jones, L. R., and Periasamy, M. (1999) *Am. J. Physiol. 276*, H89−H97.
14. Lamberth, S., Schmid, H., Muenchbach, M., Vorherr, T., Krebs, J., Carafoli, E., and Griesinger, C. (2000) *Helv. Chim. Acta 83*, 2141−2152.
15. Tatulian, S. A., Jones, L. R., Reddy, L. G., Stokes, D. L., and Tamm, L. K. (1995) *Biochemistry 34*, 4448−4456.
16. Mortishire-Smith, R. J., Pitzenberger, S. M., Burke, C. J., Middaugh, C. R., Garsky, V. M., and Johnson, R. G. (1995) *Biochemistry 34*, 7603−7613.
17. Vorherr, T., Wrzosek, A., Chiesi, M., and Carafoli, E. (1993) *Protein Sci. 2*, 339−347.
18. Kimura, Y., Kurzydlowski, K., Tada, M., and MacLennan, D. H. (1996) *J. Biol. Chem. 271*, 21726−21731.
19. Kimura, Y., Kurzydlowski, K., Tada, M., and MacLennan, D. H. (1997) *J. Biol. Chem. 272*, 15061−15064.
20. Toyofuku, T., Kurzydlowski, K., Tada, M., and MacLennan, D. H. (1994) *J. Biol. Chem. 269*, 3088−3094.
21. Toyofuku, T., Kurzydlowski, K., Tada, M., and MacLennan, D. H. (1994) *J. Biol. Chem. 269*, 22929−22932.
22. Asahi, M., Green, N. M., Kurzydlowski, K., Tada, M., and MacLennan, D. H. (2001) *Proc. Natl. Acad. Sci. U.S.A. 98*, 10061−10066.
23. Levine, B. A., Patchell, V. B., Sharma, P., Gao, Y., Bigelow, D. J., Yao, Q., Goh, S., Colyer, J., Drago, G. A., and Perry, S. V. (1999) *Eur. J. Biochem. 264*, 905−913.
24. Chen, B., and Bigelow, D. J. (2001) *Biophys. J. 80*, 35a.
25. . Yao, Q., Bevan, J. L., Weaver, R. F., and Bigelow, D. J. (1996) *Protein Expression Purif. 8*, 463−468.
26. Chen, P. S., Toribara, T. Y., and Warner, H. (1956) *Anal. Chem. 28*, 1756−1758.
27. Fernandez, J. L., Rosemblatt, M., and Hidalgo, C. (1980) *Biochim. Biophys. Acta 599*, 552−568.
28. Yao, Q., Chen, L. T., and Bigelow, D. J. (1998) *Protein Expression Purif. 13*, 191−197.
29. Lanzetta, P. A., Alvarez, L. J., Reinach, P. S., and Candia, D. A. (1979) *Anal. Biochem. 100*, 95−97.
30. Schaffner, W., and Weissmann, C. (1973) *Anal. Biochem. 56*, 502−514.
31. Fabiato, A. (1988) *Methods Enzymol. 157*, 378−417.
32. Bigelow, D. J., and Inesi, G. (1991) *Biochemistry 30*, 2113−2125.
33. Lakowicz, J. R. (1999) in *Principles of Fluorescence Spectroscopy*, 2nd ed., Kluwer Academic/Plenum Publishers, New York.
34. Hunter, G. W., and Squier, T. C. (1998) *Biochim. Biophys. Acta 1415*, 63−76.
35. Bevington, P. R. (1969) in *Data Reduction and Error Analysis for the Physical Sciences*, McGraw-Hill, New York.
36. Weber, G. (1981) *J. Phys. Chem. 85*, 949−953.
37. Peters, R., and Cherry, R. J. (1982) *Proc. Natl. Acad. Sci. U.S.A. 79*, 4317−4321.
38. Saffman, P. G., and Delbruck, M. (1975) *Proc. Natl. Acad. Sci. U.S.A. 72*, 3111−3113.
39. Birmachu, W., and Thomas, D. D. (1990) *Biochemistry 29*, 3904−3914.
40. Negash, S., Chen, L. T., Bigelow, D. J., and Squier, T. C. (1996) *Biochemistry 35*, 11247−11258.
41. Smith, S. O., Kawakami, T., Liu, W., Ziliox, M., and Aimoto, S. (2001) *J. Mol. Biol. 313*, 1139−1148.
42. Waggoner, A. S., and Stryer, L. (1970) *Proc. Natl. Acad. Sci. U.S.A. 67*, 579−589.
43. Chen, B., Jones, T. E., and Bigelow, D. J. (1999) *Biochemistry 38*, 14887−14896.
44. Steiner, R. F. (1991) in *Topics in Fluorescence Spectroscopy* (Lakowicz, J. R., Ed.) Vol. 2, pp 1−52, Plenum Press, New York.
45. Mayer, E. J., McKenna, E., Garsky, V. M., Burke, C. J., Mach, H., Middaugh, C. R., Sardana, M., Smith, J. S., and Johnson, R. G. (1996) *J. Biol. Chem. 271*, 1669−1677.
46. Ahmed, Z., Reid, D. G., Watts, A., and Middleton, D. A. (2000) *Biochim. Biophys. Acta 1468*, 187−198.
47. Pollesello, P., Annila, A., and Ovaska, M. (1999) *Biophys. J. 76*, 1784−1795.
48. Pollesello, P., and Annila, A. (2002) *Biophys. J. 83*, 484−490.
49. Arkin, I. T., Adams, P. D., Brunger, A. T., Smith, S. O., and Engelman, D. M. (1997) *Annu. Rev. Biophys. Biomol. Struct. 26*, 157−179.
50. Karim, C. B., Marquardt, C. G., Stamm, J. D., Barany, G., and Thomas, D. D. (2000) *Biochemistry 39*, 10892−10897.
51. Li, H., Cocco, M. J., Steitz, T. A., and Engelman, D. M. (2001) *Biochemistry 40*, 6636−6645.
52. Simmerman, H. K., Kobayashi, Y., Autry, J. M., and Jones, L. R. (1996) *J. Biol. Chem. 271*, 5941−5946.
53. Cornea, R. L., Jones, L. R., Autry, J. M., and Thomas, D. D. (1997) *Biochemistry 36*, 2960−2967.
54. Reddy, L. G., Jones, L. R., and Thomas, D. D. (1999) *Biochemistry 38*, 3954−3962.
55. Thomas, D. D., Reddy, L. G., Karim, C. B., Li, M., Cornea, R., Autry, J. M., Jones, L. R., and Stamm, J. (1998) *Ann. N.Y. Acad. Sci. 853*, 186−194.
56. Bers, D. M. (2001) *Excitation-Contraction Coupling and Cardiac Contractile Force*, 2nd ed., Kluwer Academic Publishers, Dordrecht, The Netherlands.
57. Jones, L. R., Cornea, R. L., and Chen, Z. (2002) *J. Biol. Chem. 277*, 28319−28329.
58. Negash, S., Huang, S., and Squier, T. C. (1999) *Biochemistry 38*, 8150−8158.
59. Cantilina, T., Sagara, Y., Inesi, G., and Jones, L. R. (1993) *J. Biol. Chem. 268*, 17018−17025.

BI0266030